

Diboson (including di-Higgs) at FCC-hh

Shankha Banerjee
CERN

January 27, 2023



Why FCC-hh and why dibosons?

- To push the field of particle physics to the **next energy frontier beyond HL-LHC** → increasing possible mass probe of BSM particles by an order of magnitude
- To push precision by several orders of magnitude thereby constraining EFT couplings and gauging the presence of possible new physics effects
- Diboson (W^+W^- , $W^\pm Z$, ZZ , $W^\pm\gamma$) searches → **TGC** and QGC couplings
- Higgs-strahlung (Zh , $W^\pm h$) searches → **TGC**, VVh , and **contact ($q\bar{q}^{(\prime)}Vh$) interactions** [See talks by Ang Li and Giovanni Marchiori for Zh in e^+e^- colliders]
- Di-Higgs (hh , $hh + j$, $hh + jj$, $t\bar{t}hh$) searches → **Higgs trilinear**, Higgs quartic, $t\bar{t}hh$ couplings [See slides by Michele Selvaggi, Jorge de Blas, and Ennio Salvioni]
[For top-Higgs interplay and global fits see talk by Eleni Vryonidou]

Cross-section growth with $\sqrt{\hat{s}}$ in VV, Vh, hh

	$\sigma_{LO}(\text{pb})$	$\sigma_{NLO}(\text{pb})$	$\sigma_{NLO} + \sigma_{gg}(\text{pb})$	$\sigma_{NNLO}(\text{pb})$
100 TeV				
$ZZ \rightarrow e^+e^-\mu^+\mu^-$	0.29	0.37	0.43	0.460 (+4.0%) (-3.3%)
$WW \rightarrow e\nu\mu\nu$	10.0	13.4	14.4	15.8 (+3.6%) (-3.0%)
$WZ \rightarrow e\nu\mu^+\mu^-$	1.1	2.2	-	$2.38 \pm 2.3\%$
27 TeV				
$ZZ \rightarrow e^+e^-\mu^+\mu^-$	0.058	0.080	0.090	0.0952 (+2.9%) (-2.4%)
$WW \rightarrow e\nu\mu\nu$	2.1	3.0	3.2	3.46 (+2.8%) (-2.4%)
$WZ \rightarrow e\nu\mu^+\mu^-$	0.23	0.42	-	$0.483 \pm 2.1\%$

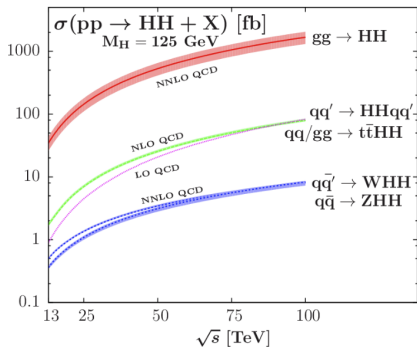
	$gg \rightarrow H$	VBF	WH	ZH	$t\bar{t}H$	HH
N_{100}	24×10^9	2.1×10^9	4.6×10^8	3.3×10^8	9.6×10^8	3.6×10^7
N_{100}/N_{14}	180	170	100	110	530	390
N_{27}	2.2×10^9	1.8×10^8	5.1×10^7	3.7×10^7	4.4×10^7	2.1×10^6
N_{27}/N_{14}	16	15	11	12	24	19

- For $W^+W^-(W^\pm Z)$, there is a growth of $\sim 8.7(9.5)$ when going from 14 TeV to 100 TeV in the SM. For ZZ , it is ~ 9.6 .

[FCC Physics Opportunities: CDR; 2018]

Cross-section growth with $\sqrt{\hat{s}}$ in $hh + X$

	$\sigma[100 \text{ TeV}](\text{fb})$	$\sigma[27 \text{ TeV}](\text{fb})$
$gg \rightarrow HH$	$1.22 \times 10^3 \begin{smallmatrix} +0.9\% \\ -3.2\% \end{smallmatrix} \pm 2.4\% \pm 4.5\%_{m_t}$	$140 \begin{smallmatrix} +1.3\% \\ -3.9\% \end{smallmatrix} \pm 2.5\% \pm 3.4\%_{m_t}$
$HHjj$	$80.5 \pm 0.5\% \pm 1.8\%$	$1.95 \pm 2\% \pm 2.4\%$
W^+HH	$4.7 \pm 1\% \pm 1.8\%$	$0.37 \pm 0.4\% \pm 2.1\%$
W^-HH	$3.3 \pm 4\% \pm 1.9\%$	$0.20 \pm 1.3\% \pm 2.7\%$
ZHH	$8.2 \pm 5\% \pm 1.7\%$	$0.41 \pm 3\% \pm 1.8\%$
$\bar{u}HH$	$82.1 \pm 8\% \pm 1.6\%$	$0.95 \begin{smallmatrix} +1.7\% \\ -4.5\% \end{smallmatrix} \pm 3.1\%$



[FCC Physics Opportunities: CDR; 2018], [Baglio, Djouadi, Quevillon; 2015]

EFT motivation

- Many reasons to go beyond the SM, viz. **gauge hierarchy**, **neutrino mass**, **dark matter**, **baryon asymmetry** etc.
- Plethora of BSM theories to address these issues
- Two phenomenological approaches:
 - *Model dependent*: study the signatures of each model individually
 - *Model independent*: **low energy effective theory formalism**
- The SM here is a low energy effective theory **valid below a cut-off scale Λ**
- A bigger theory (**either weakly or strongly coupled**) is assumed to supersede the SM above the scale Λ
- At the perturbative level, all heavy ($> \Lambda$) DOF are decoupled from the low energy theory [[See Dave Sutherland's slides on SMEFT versus HEFT](#)]
- Appearance of HD operators in the effective Lagrangian valid below Λ

$$\mathcal{L} = \mathcal{L}_{SM}^{d=4} + \sum_{d \geq 5} \sum_i \frac{f_i}{\Lambda^{d-4}} \mathcal{O}_i^d$$

SMEFT motivation

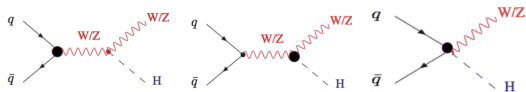
- Precisely measuring the Higgs couplings → one of the most important LHC goals and that of the FCC-hh as well
- Indirect constraints can constrain much higher scales S , T parameters being prime examples
- Q: How well does the FCC-hh compete with LEP in constraining precision physics?
A: From EFT correlated variables, LEP already constrained certain anomalous Higgs couplings → Z -pole measurements, TGCs
Going to higher energies in FCC-hh is the only way to obtain newer information after the HL-LHC
- EFT techniques show that many Higgs deformations aren't independent from cTGCs and EW precision which were already constrained at LEP → Same operators affect TGCs and Higgs deformations

Diboson and Higgs-strahlung in SMEFT

$\mathcal{O}_{H\Box} = (H^\dagger H)\Box(H^\dagger H)$	$\mathcal{O}_{HL}^{(3)} = iH^\dagger \sigma^a \overleftrightarrow{D}_\mu H \bar{L} \sigma^a \gamma^\mu L$
$\mathcal{O}_{HD} = (H^\dagger D_\mu H)^*(H^\dagger D_\mu H)$	$\mathcal{O}_{HB} = H ^2 B_{\mu\nu} B^{\mu\nu}$
$\mathcal{O}_{Hu} = iH^\dagger \overleftrightarrow{D}_\mu H \bar{u}_R \gamma^\mu u_R$	$\mathcal{O}_{HWB} = H^\dagger \sigma^a H W_{\mu\nu}^a B^{\mu\nu}$
$\mathcal{O}_{Hd} = iH^\dagger \overleftrightarrow{D}_\mu H \bar{d}_R \gamma^\mu d_R$	$\mathcal{O}_{HW} = H ^2 W_{\mu\nu} W^{\mu\nu}$
$\mathcal{O}_{He} = iH^\dagger \overleftrightarrow{D}_\mu H \bar{e}_R \gamma^\mu e_R$	$\mathcal{O}_{H\tilde{B}} = H ^2 B_{\mu\nu} \tilde{B}^{\mu\nu}$
$\mathcal{O}_{HQ}^{(1)} = iH^\dagger \overleftrightarrow{D}_\mu H \bar{Q} \gamma^\mu Q$	$\mathcal{O}_{H\tilde{W}B} = H^\dagger \sigma^a H W_{\mu\nu}^a \tilde{B}^{\mu\nu}$
$\mathcal{O}_{HQ}^{(3)} = iH^\dagger \sigma^a \overleftrightarrow{D}_\mu H \bar{Q} \sigma^a \gamma^\mu Q$	$\mathcal{O}_{H\tilde{W}} = H ^2 W_{\mu\nu}^a \tilde{W}^{a\mu\nu}$
$\mathcal{O}_{HL}^{(1)} = iH^\dagger \overleftrightarrow{D}_\mu H \bar{L} \gamma^\mu L$	$\mathcal{O}_{y_b} = H ^2 (\bar{Q}_3 H b_R + h.c.)$

Operators in the Warsaw basis contributing to anomalous $q\bar{q}^{(')} \rightarrow WV, Vh$ processes

Diboson and Higgs-strahlung in SMEFT



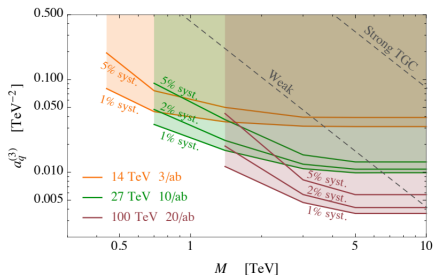
[Franceschini, Panico, Pomarol, Riva, Wulzer; 2017], [SB, Gupta, Reiness, Seth, Spannowsky; 2020]

$$\begin{aligned}
 \Delta\mathcal{L}_6 \supset & \delta\hat{g}_{WW}^h \frac{2m_W^2}{v} h W^{+\mu} W_{\mu}^- + \delta\hat{g}_{ZZ}^h \frac{2m_Z^2}{v} h \frac{Z^\mu Z_\mu}{2} + \delta g_Q^W (W_\mu^+ \bar{u}_L \gamma^\mu d_L + h.c.) \\
 & + \delta g_L^W (W_\mu^+ \bar{\nu}_L \gamma^\mu e_L + h.c.) + g_{WL}^h \frac{h}{v} (W_\mu^+ \bar{\nu}_L \gamma^\mu e_L + h.c.) \\
 & + g_{WQ}^h \frac{h}{v} (W_\mu^+ \bar{u}_L \gamma^\mu d_L + h.c.) + \sum_f \delta g_f^Z Z_\mu \bar{f} \gamma^\mu f + \sum_f g_{Zf}^h \frac{h}{v} Z_\mu \bar{f} \gamma^\mu f \\
 & + \kappa_{WW} \frac{h}{v} W^{+\mu\nu} W_{\mu\nu}^- + \tilde{\kappa}_{WW} \frac{h}{v} W^{+\mu\nu} \tilde{W}_{\mu\nu}^- + \kappa_{ZZ} \frac{h}{2v} Z^{\mu\nu} Z_{\mu\nu} \\
 & + \tilde{\kappa}_{ZZ} \frac{h}{2v} Z^{\mu\nu} \tilde{Z}_{\mu\nu} + \kappa_{Z\gamma} \frac{h}{v} A^{\mu\nu} Z_{\mu\nu} \\
 & + \tilde{\kappa}_{Z\gamma} \frac{h}{v} A^{\mu\nu} \tilde{Z}_{\mu\nu} + \delta\hat{g}_{bb}^h \frac{\sqrt{2}m_b}{v} h b \bar{b} \\
 & + igc_{\theta_W} \delta g_1^Z [Z^\mu (W^{+\nu} W_{\nu\mu}^- - h.c.) + Z^{\mu\nu} (W_\mu^+ W_\nu^-) + \dots] \\
 & + ie\delta\kappa_\gamma [(A^{\mu\nu} - c_{\theta_W} Z^{\mu\nu}) W_\mu^+ W_{\nu}^- + \dots]
 \end{aligned}$$

Diboson example: $W^\pm Z$

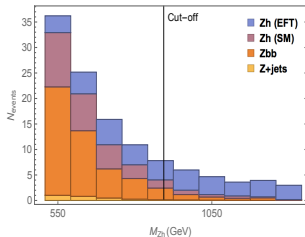
[Franceschini, Panico, Pomarol, Riva, Wulzer; 2017]

- Process: $pp \rightarrow W^\pm Z + \text{jets} \rightarrow \ell\nu\ell'\bar{\ell}' + \text{jets}$ with $\ell, \ell' = e, \mu$
- Low reducible background. Systematic uncertainty of 5% considered
- LO matched with one extra jet
- Sensitivity of high-energy primary $a_q^{(3)} = 4 \frac{C_{HL}^{(3)}}{M^2}$ ("Weak" "non-universal" theories) is studied at various energies
- Result: HL-LHC, 3 ab^{-1} : $a_q^{(3)} \in [-4.9, 3.9]10^{-2} \text{ TeV}^{-2}$ and FCC-hh, 20 ab^{-1} : $a_q^{(3)} \in [-7.3, 5.7]10^{-3} \text{ TeV}^{-2}$



Differential in Energy: $pp \rightarrow Zh$ at high energies (Contact term) at HL-LHC

- We study the impact of constraining TGC couplings at higher energies
- We study the channel $pp \rightarrow Zh \rightarrow \ell^+ \ell^- b\bar{b}$
- The backgrounds are SM $pp \rightarrow Zh, Zb\bar{b}, t\bar{t}$ and the fake $pp \rightarrow Zjj$ ($j \rightarrow b$ fake rate taken as 2%)
- Major background $Zb\bar{b}$ (b -tagging efficiency taken to be 70%)
- Boosted substructure analysis with fat-jets of $R = 1.2$ used



Cuts	Zbb	Zh (SM)
At least 1 fat jet with 2 B -mesons with $p_T > 15$ GeV	0.52	0.79
2 OSSF isolated leptons	0.44	0.48
$80 \text{ GeV} < M_{\ell\ell} < 100 \text{ GeV}$, $p_{T,\ell\ell} > 260 \text{ GeV}$, $\Delta R_{\ell\ell} > 0.2$	0.83	0.84
At least 1 fat jet with 2 B -meson tracks with $p_T > 220 \text{ GeV}$	0.85	0.94
2 Mass drop subjets and ≥ 2 filtered subjets	0.88	0.92
2 b -tagged subjets	0.35	0.40
$115 \text{ GeV} < m_h < 135 \text{ GeV}$	0.180	0.50
$\Delta R(b_i, \ell_j) > 0.4$, $\cancel{E}_T < 30 \text{ GeV}$, $ y_h < 2.5$, $p_{T,h/Z} > 300 \text{ GeV}$	0.31	0.55

Bounds on Pseudo-observables at HL-LHC and FCC-hh

HL-LHC: @ 95% CL

$$g_{Zp}^h \in [-0.004, 0.004] \quad (300 \text{ fb}^{-1})$$

$$g_{Zp}^h \in [-0.001, 0.001] \quad (3000 \text{ fb}^{-1})$$

Directions: ($\xi = v^2/\Lambda^2$) [Araz, SB, Gupta, Spannowsky, 2020]

$$|(-0.04 c_Q^1 + 1.4 c_Q^{(3)} + 0.1 c_{uR} - 0.03 c_{dR})\xi| < 0.003 \quad [VBF]$$

$$|(-0.18 c_Q^1 + 1.3 c_Q^{(3)} + 0.3 c_{uR} - 0.1 c_{dR})\xi| < 0.0005 \quad [Zh]$$

$$|c_Q^{(3)}\xi| < 0.0004 \quad [Wh]$$

$$-0.0004 < c_Q^{(3)}\xi < 0.0003 \quad [WZ]$$

FCC-hh: @ 95% CL

$$g_{Zp}^{h,\ell\ell b\bar{b}} \in [-0.00051, 0.00054] \quad ([-0.00021, 0.00023]) \text{ with 5\% systematic uncertainty.}$$

$$\in [-0.00047, 0.00049] \quad ([-0.00016, 0.00017]) \text{ with 1\% systematic uncertainty.}$$

$$g_{Zp}^{h,\ell\ell\gamma\gamma} \in [-0.001, 0.001] \quad ([-0.0004, 0.0004]) \text{ with 1\% systematic uncertainty at 3 (30) ab}^{-1}.$$

	Our 100 TeV Projection	Our 14 TeV projection	LEP Bound
δg_{uL}^Z	$\pm 0.0003 (\pm 0.0001)$	$\pm 0.002 (\pm 0.0007)$	-0.0026 ± 0.0032
δg_{dL}^Z	$\pm 0.0003 (\pm 0.0001)$	$\pm 0.003 (\pm 0.001)$	0.0023 ± 0.002
δg_{uR}^Z	$\pm 0.0005 (\pm 0.0002)$	$\pm 0.005 (\pm 0.001)$	-0.0036 ± 0.0070
δg_{dR}^Z	$\pm 0.0015 (\pm 0.0006)$	$\pm 0.016 (\pm 0.005)$	0.016 ± 0.0104
δg_1^Z	$\pm 0.0005 (\pm 0.0002)$	$\pm 0.005 (\pm 0.001)$	$-0.009^{+0.043}_{-0.042}$
$\delta \kappa_\gamma$	$\pm 0.0035 (\pm 0.0015)$	$\pm 0.032 (\pm 0.009)$	$-0.016^{+0.085}_{-0.096}$
\hat{S}	$\pm 0.0035 (\pm 0.0015)$	$\pm 0.032 (\pm 0.009)$	0.0004 ± 0.0007
W	$\pm 0.0004 (\pm 0.0002)$	$\pm 0.003 (\pm 0.001)$	-0.0003 ± 0.0006
Y	$\pm 0.0035 (\pm 0.0015)$	$\pm 0.032 (\pm 0.009)$	0.0000 ± 0.0006

[SB, Englert, Gupta, Spannowsky, 2018] LEP bounds: [Falkowski, Riva, 2014], [Baak et al., 2012], [Barbieri, Pomarol, Rattazzi, Strumia, 2004]

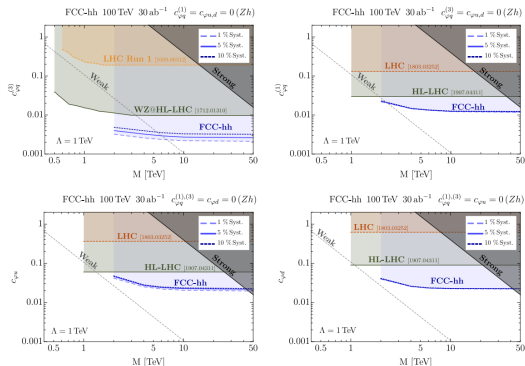
Map between bases: Zh case contact interaction h_{Zf}^h

	EFT directions probed by high energy $ff \rightarrow Vh$ production
Warsaw basis [1]	$-\frac{2g}{c_{\theta_W}} \frac{v^2}{\Lambda^2} (T_3^f c_L^1 - T_3^f c_L^3 + (1/2 - T_3^f) c_f)$
BSM primaries [2]	$\frac{2g}{c_{\theta_W}} Y_f t_{\theta_W}^2 \delta\kappa_\gamma + 2\delta g_f^Z - \frac{2g}{c_{\theta_W}} (T_3^f c_{\theta_W}^2 + Y_f s_{\theta_W}^2) \delta g_1^Z$
SILH Lagrangian [26]	$\frac{g}{c_{\theta_W}} \frac{m_W^2}{\Lambda^2} (2T_3^f \hat{c}_W - 2t_{\theta_W}^2 Y_f \hat{c}_B)$
Universal observables	$\frac{2g}{c_{\theta_W}} Y_f t_{\theta_W}^2 (\delta\kappa_\gamma - \hat{S} + Y) - \frac{2g}{c_{\theta_W}} (T_3^f c_{\theta_W}^2 + Y_f s_{\theta_W}^2) \delta g_1^Z - \frac{2g}{c_{\theta_W}} T_3^f W$
High energy primaries [20]	$-\frac{2m_W^2}{g c_{\theta_W}} (T_3^f a_q^{(1)} - T_3^f a_q^{(3)} + (1/2 - T_3^f) a_f)$

Here $\hat{c}_W = c_W + c_{HW} - c_{2W}$ and $\hat{c}_B = c_B + c_{HB} - c_{2B}$.

[SB, Englert, Gupta, Spannowsky, 2018]

$Zh \rightarrow \ell^+ \ell^- (\nu \bar{\nu}) \gamma \gamma$ at FCC-hh



Single-operator analysis (growth \hat{s})

$$c_{\varphi q}^{(3)} = + \frac{\Lambda^2}{4m_W^2} g^2 \left(\delta g_L^{Zu} - \delta g_L^{Zd} - c_W^2 \delta g_{1z} \right)$$

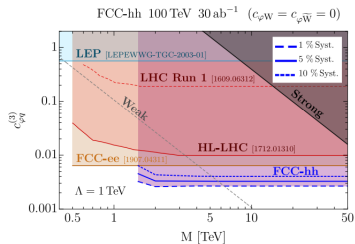
$$c_{\varphi q}^{(1)} = - \frac{\Lambda^2}{4m_W^2} g^2 \left(\delta g_L^{Zu} + \delta g_L^{Zd} + \frac{1}{3} (t_W^2 \delta \kappa_\gamma - s_W^2 \delta g_{1z}) \right)$$

$$c_{\varphi u} = - \frac{\Lambda^2}{2m_W^2} g^2 \left(\delta g_R^{Zu} + \frac{2}{3} (t_W^2 \delta \kappa_\gamma - s_W^2 \delta g_{1z}) \right)$$

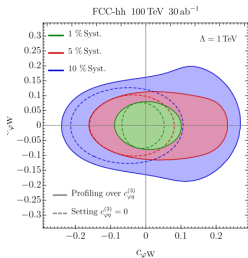
$$c_{\varphi d} = - \frac{\Lambda^2}{2m_W^2} g^2 \left(\delta g_R^{Zd} - \frac{1}{3} (t_W^2 \delta \kappa_\gamma - s_W^2 \delta g_{1z}) \right)$$

[Bishara, De Curtis, Rose, Englert, Grojean, Montull, Panico, Rossia; 2021]

$Wh \rightarrow l\nu\gamma$ at FCC-hh



Single-operator analysis (growth \hat{s} , longitudinal) [Bishara, Englert, Grojean, Montull, Panico, Rossia; 2020]



(growth $\sqrt{\hat{s}}$, profiled over $\mathcal{O}_{HQ}^{(3)}$, transverse)

Top interaction with Higgs and EW bosons (FCC-hh)

- $Zt_R\bar{t}_R$, $hZt_R\bar{t}_R$ poorly constrained from LEP via Z -boson decays
- Understanding top couplings to EW bosons is well-motivated as top and its partners can play crucial role in EWSB by radiatively contributing to the Higgs potential
- $\Lambda_{\text{top partners}} \sim \mathcal{O}(\text{TeV})$ from naturalness considerations \rightarrow Sizeable indirect effects

- In composite models, integrating out top partners can lead to the following operators

$$\mathcal{O}_{HQL}^{(1)} = iH^\dagger \overleftrightarrow{D}_\mu H \bar{Q}_L \gamma^\mu Q_L \quad \mathcal{O}_{HQL}^{(3)} = iH^\dagger \sigma^a \overleftrightarrow{D}_\mu H \bar{Q}_L \sigma^a \gamma^\mu Q_L \quad \mathcal{O}_{HtR} = iH^\dagger \overleftrightarrow{D}_\mu H \bar{t}_R \gamma^\mu t_R$$

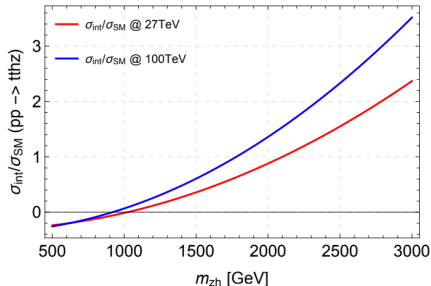
- Operators involving left-chiral fermions deform both $Zb\bar{b}$ and $Zt\bar{t}$ \rightarrow constrained by Z -pole and TGCs
- \mathcal{O}_{HtR} is unconstrained. Expanding in unitary gauge

$$\frac{\mathcal{O}_{HtR}}{\Lambda^2} = -\frac{gv^2}{2c_{\theta_W}\Lambda^2} \left(1 + \frac{2h}{v} + \frac{h^2}{v^2}\right) Z_\mu \bar{t}_R \gamma^\mu t_R$$

[SB, Gupta, Jain, Mangano, Venturini; in preparation], Les Houches 2019 WG report

Top interaction with Higgs and EW bosons (FCC-hh)

- In SM, $\sigma_{gg \rightarrow t\bar{t}hZ} \sim 1.5(130)$ fb at 14 TeV (100 TeV). With $m_{Zh} > 1.5$ TeV
 $\sigma_{gg \rightarrow t\bar{t}hZ} \sim 3.6$ fb at 100 TeV \rightarrow Potential to study fully leptonic final state
- Final state: 4 b -tagged jets, 3 leptons, 2 light jets and \cancel{E}_T
- Backgrounds, viz., $t\bar{t}h$ + jets, $t\bar{t}Z$ + jets, $t\bar{t}hb\bar{b}$, $t\bar{t}Zb\bar{b}$, $t\bar{t}hh$, $t\bar{t}WZ$ + jets, VVV + jets, $WZb\bar{b}$ + jets
- Treating SM $t\bar{t}hZ$ as signal, $S/B \sim 0.20$ and preliminary bound on $|g_{hZt_R}| \sim \mathcal{O}(10^{-3})$



[SB, Gupta, Jain, Mangano, Venturini; in preparation], Les Houches 2019 WG report

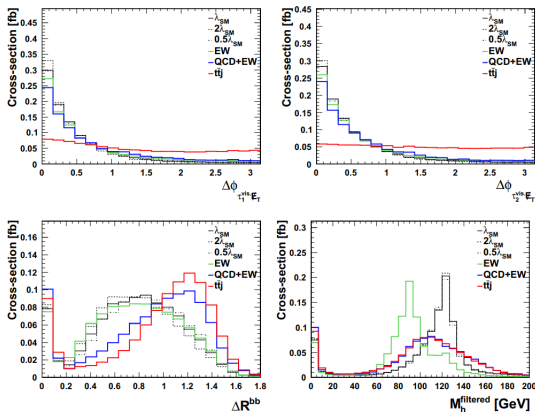
Di-Higgs + jet at FCC-hh

- Observing the Higgs self-coupling at the HL-LHC seem difficult at the moment
- Di-Higgs cross-section increases by **39 times** going from 14 TeV \rightarrow 100 TeV
- Extra jet emission becomes significantly less suppressed: **77 times** enhancement from 14 TeV \rightarrow 100 TeV collider \rightarrow **extra handle**
- Recoiling a collimated Higgs pair against a jet exhibits extra sensitivity (decorrelates $p_{T,h}$ and m_{hh}) to λ_{hhh}
- Use substructure technique: BDRS [Butterworth, *et. al.*; 2008] with **mass drop** and **filtering**

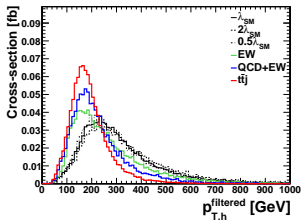
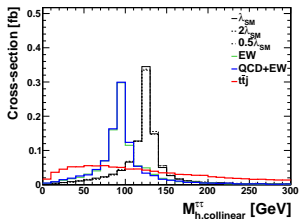
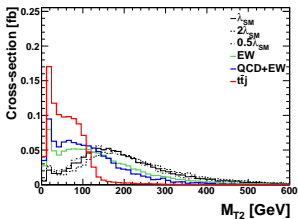
[SB, Englert, Mangano, Selvaggi, Spannowsky; 2018]

Di-Higgs + jet at FCC-hh ($jb\bar{b}\tau^+\tau^-$)

- $R = 1.5$, $p_T^j > 110$ GeV, τ -tag efficiency 70%, b -tag efficiency 70%, b -mistag rate 2%;
Combined $\mathcal{T}_{h\mathcal{T}h}$ and $\mathcal{T}_{h\mathcal{T}\ell}$
- Backgrounds: EW (example: $HZ/\gamma^* + \text{jet}$), QCD+EW (Example: $b\bar{b}Z/\gamma^* + \text{jet}$), $t\bar{t} + \text{jet}$



Di-Higgs + jet at FCC-hh ($j b \bar{b} \tau^+ \tau^-$)



Di-Higgs + jet at FCC-hh ($jb\bar{b}\tau^+\tau^-$)

	signal [fb]	QCD+QED [fb]	QED [fb]	$t\bar{t}j$ [fb]	tot. background [fb]	S/B	S/\sqrt{B} , 30/ab
$\kappa_\lambda = 0.5$	0.428	0.95	0.27	2.31	3.53	0.121	39.44
$\kappa_\lambda = 1$	0.363					0.103	33.44
$\kappa_\lambda = 2$	0.264					0.075	24.31

$$0.76 < \kappa_\lambda < 1.28 \quad 3/\text{ab}$$

$$0.92 < \kappa_\lambda < 1.08 \quad 30/\text{ab}$$

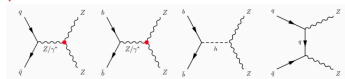
at 68% confidence level using the CLs method.

[SB, Englert, Mangano, Selvaggi, Spannowsky; 2018]

Diboson example: ZZ

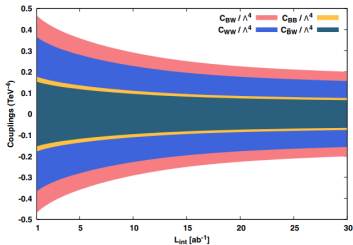
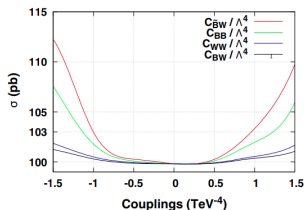
- ZZ, Z γ channels let us constrain the **neutral anomalous TGCs** which appear from **D8 operators**

- For ZZ, relevant operators are $\mathcal{O}_{\tilde{B}W} = iH^\dagger \tilde{B}_{\mu\nu} W^{\mu\rho} D_\rho D^\nu H$ (*CP*-conserving), $\mathcal{O}_{BW} = iH^\dagger B_{\mu\nu} W^{\mu\rho} D_\rho D^\nu H$, $\mathcal{O}_{WW} = iH^\dagger W_{\mu\nu} W^{\mu\rho} D_\rho D^\nu H$, and



$$\mathcal{O}_{BB} = iH^\dagger B_{\mu\nu} B^{\mu\rho} D_\rho D^\nu H \text{ (Last three } CP\text{-violating)}$$

- Studying one coupling at a time in the 4ℓ channel, the bounds are an order stronger than HL-LHC results in the 4ℓ channel



[Yilmaz1, Senol, Denizli, Cakir, Cakir; 2019]

Summary and conclusions

- FCC-hh will be an extremely fertile ground to search for new physics including precision physics in the diboson, Higgs-strahlung, and di-Higgs sectors.
- For WZ production, the improvement on $C_{HL}^{(3)}$ is $\sim 85\%$ in the fully leptonic channel.
- Detailed studies need to be performed for W^+W^- , and $W^\pm\gamma$ at FCC-hh.
- For Zh , the contact interactions gain improvements between 80% and 90% ($\sim 50\%$) in the $b\bar{b}l^+l^-$ ($\gamma\gamma l^+l^-$) channel.
- For $hh + \text{jet}$, κ_λ is constrained to 8%. Marginalising over all other relevant EFT couplings necessary.
- One operator at a time study of aNTGCs puts constraints of an order stronger. Necessary to do a global analysis including contact interactions with fermions.

Backup Slides

Higgs Pseudo-Observables

- Following are some of the **Higgs observables** (assuming flavour universality)

$$hW_{\mu\nu}^+ W^{-\mu\nu}$$

$$hZ_{\mu\nu} Z^{\mu\nu}, hA_{\mu\nu} A^{\mu\nu}, hA_{\mu\nu} Z^{\mu\nu}, hG_{\mu\nu} G^{\mu\nu}$$

$$hf\bar{f}, h^2f\bar{f}$$

$$hW_{\mu}^+ W^{-\mu}$$

$$h^3$$

$$hZ_{\mu}\bar{f}_{L,R}\gamma^{\mu}f_{L,R}$$

- These anomalous Higgs couplings are first probed at the LHC

Electroweak Pseudo-Observables

- Following are the **9 EW precision observables** (assuming flavour universality)

$$Z_\mu \bar{f}_{L,R} \gamma^\mu f_{L,R} \quad W_\mu^+ \bar{u}_L \gamma^\mu d_R$$

- These couplings were measured very precisely by the Z/W -pole measurements through the Z/W decays

- Following are the **3 TGCs** which were measured by the $e^+e^- \rightarrow W^+W^-$ channel at LEP

$$g_1^Z c_{\theta_w} Z^\mu (W^{+\nu} \hat{W}_{\mu\nu}^- - W^{-\nu} \hat{W}_{\mu\nu}^+)$$

$$k_\gamma s_{\theta_w} \hat{A}^{\mu\nu} W_\mu^+ W_\nu^-$$

$$\lambda_\gamma s_{\theta_w} \hat{A}^{\mu\nu} W_\mu^{-\rho} W_{\rho\nu}^+$$

- Finally, following are the **QGCs**

$$Z^\mu Z^\nu W_\mu^- W_\nu^+$$

$$W^{-\mu} W^{+\nu} W_\mu^- W_\nu^+$$

Effective Field Theory: The operators at play

- There are only **18 independent operators** from which the aforementioned vertices ensue

$\mathcal{O}_H = \frac{1}{2}(\partial^\mu H ^2)^2$ $\mathcal{O}_T = \frac{1}{2} \left(H^\dagger \overleftrightarrow{D}_\mu H \right)^2$ $\mathcal{O}_6 = \lambda H ^6$
$\mathcal{O}_W = \frac{ig}{2} \left(H^\dagger \sigma^a \overleftrightarrow{D}_\mu H \right) D^\nu W_{\mu\nu}^a$ $\mathcal{O}_B = \frac{ig'}{2} \left(H^\dagger \overleftrightarrow{D}_\mu H \right) \partial^\nu B_{\mu\nu}$

$\mathcal{O}_{BB} = g'^2 H ^2 B_{\mu\nu} B^{\mu\nu}$ $\mathcal{O}_{GG} = g_s^2 H ^2 G_{\mu\nu}^A G^{A\mu\nu}$ $\mathcal{O}_{HW} = ig(D^\mu H)^\dagger \sigma^a (D^\nu H) W_{\mu\nu}^a$ $\mathcal{O}_{HB} = ig'(D^\mu H)^\dagger (D^\nu H) B_{\mu\nu}$ $\mathcal{O}_{3W} = \frac{1}{3!} g \epsilon_{abc} W_\mu^{a\nu} W_{\nu\rho}^b W^{c\rho\mu}$
--

$\mathcal{O}_{y_u} = y_u H ^2 \bar{Q}_L \tilde{H} u_R$	$\mathcal{O}_{y_d} = y_d H ^2 \bar{Q}_L H d_R$	$\mathcal{O}_{y_e} = y_e H ^2 \bar{L}_L H e_R$
$\mathcal{O}_R^u = (iH^\dagger \overleftrightarrow{D}_\mu H)(\bar{u}_R \gamma^\mu u_R)$	$\mathcal{O}_R^d = (iH^\dagger \overleftrightarrow{D}_\mu H)(\bar{d}_R \gamma^\mu d_R)$	$\mathcal{O}_R^e = (iH^\dagger \overleftrightarrow{D}_\mu H)(\bar{e}_R \gamma^\mu e_R)$
$\mathcal{O}_L^q = (iH^\dagger \overleftrightarrow{D}_\mu H)(\bar{Q}_L \gamma^\mu Q_L)$		
$\mathcal{O}_L^{(3)q} = (iH^\dagger \sigma^a \overleftrightarrow{D}_\mu H)(\bar{Q}_L \sigma^a \gamma^\mu Q_L)$		

Effective Field Theory: The operators at play

- There are 18 independent operators and many more pseudo-observables
- This implies correlations between the various pseudo-observables
- Besides, the following operators can not be constrained by LEP

$$|H|^2 G_{\mu\nu} G^{\mu\nu}, |H|^2 B_{\mu\nu} B^{\mu\nu}, |H|^2 W_{\mu\nu}^a W^{a,\mu\nu}$$

$$|H|^2 |D_\mu H|^2, |H|^6$$

$$|H|^2 f_L H f_R + h.c.$$

- It is thus necessary to redefine many parameters, viz.,

$$e(\hat{h}), s_{\theta_w}(\hat{h}), g_s(\hat{h}), \lambda_h(\hat{h}), Z_h(\hat{h}), Y_f(\hat{h}),$$

$$\text{where } \hat{h} = v + h$$

Higgs anomalous couplings: Dimension 6 effects

$$\begin{aligned}\mathcal{L}_h^{\text{primary}} &= g_{VV}^h h \left[W^{+\mu} W_{\mu}^{-} + \frac{1}{2c_{\theta_W}^2} Z^{\mu} Z_{\mu} \right] + g_{3h} h^3 + g_{ff}^h (h \bar{f}_L f_R + h.c.) \\ &+ \kappa_{GG} \frac{h}{v} G^{A\mu\nu} G_{\mu\nu}^A + \kappa_{\gamma\gamma} \frac{h}{v} A^{\mu\nu} A_{\mu\nu} + \kappa_{Z\gamma} t_{\theta_W} \frac{h}{v} A^{\mu\nu} Z_{\mu\nu},\end{aligned}$$

$$\begin{aligned}\Delta\mathcal{L}_h &= \delta g_{ZZ}^h \frac{v}{2c_{\theta_W}^2} h Z^{\mu} Z_{\mu} + g_{Zff}^h \frac{h}{2v} (Z_{\mu} J_N^{\mu} + h.c.) + g_{Wff'}^h \frac{h}{v} (W_{\mu}^{+} J_C^{\mu} + h.c.) \\ &+ \kappa_{WW} \frac{h}{v} W^{+\mu\nu} W_{\mu\nu}^{-} + \kappa_{ZZ} \frac{h}{v} Z^{\mu\nu} Z_{\mu\nu},\end{aligned}$$

[Pomarol, 2014]

- Higgs interactions were directly measured for the first time at the LHC

STU oblique parameters



$$\Pi_{\gamma\gamma}(q^2) = q^2 \Pi'_{\gamma\gamma}(0) + \dots$$

$$\Pi_{Z\gamma}(q^2) = q^2 \Pi'_{Z\gamma}(0) + \dots$$

$$\Pi_{ZZ}(q^2) = \Pi_{ZZ}(0) + q^2 \Pi'_{ZZ}(0) + \dots$$

$$\Pi_{WW}(q^2) = \Pi_{WW}(0) + q^2 \Pi'_{WW}(0) + \dots$$

$$\alpha S = 4s_w^2 c_w^2 \left[\Pi'_{ZZ}(0) - \frac{c_w^2 - s_w^2}{s_w c_w} \Pi'_{Z\gamma}(0) - \Pi'_{\gamma\gamma}(0) \right]$$

$$\alpha T = \frac{\Pi_{WW}(0)}{M_W^2} - \frac{\Pi_{ZZ}(0)}{M_Z^2}$$

$$\alpha U = 4s_w^2 \left[\Pi'_{WW}(0) - c_w^2 \Pi'_{ZZ}(0) - 2s_w c_w \Pi'_{Z\gamma}(0) - s_w^2 \Pi'_{\gamma\gamma}(0) \right]$$

1. Any BSM correction which is indistinguishable from a redefinition of e , G_F and M_Z (or equivalently, g_1 , g_2 and v) in the Standard Model proper at the **tree level** does not contribute to S, T or U.
2. Assuming that the **Higgs sector** consists of electroweak doublet(s) H, the effective action term $|H^\dagger D_\mu H|^2 / \Lambda^2$ only contributes to T and not to S or U. This term violates **custodial symmetry**.
3. Assuming that the **Higgs sector** consists of electroweak doublet(s) H, the effective action term $H^\dagger W^{\mu\nu} B_{\mu\nu} H / \Lambda^2$ only contributes to S and not to T or U. (The contribution of $H^\dagger B^{\mu\nu} B_{\mu\nu} H / \Lambda^2$ can be absorbed into g_1 and the contribution of $H^\dagger W^{\mu\nu} W_{\mu\nu} H / \Lambda^2$ can be absorbed into g_2).
4. Assuming that the **Higgs sector** consists of electroweak doublet(s) H, the effective action term $(H^\dagger W^{\mu\nu} H) (H^\dagger W_{\mu\nu} H) / \Lambda^4$ contributes to U.

ZH: Four directions in the EFT space (SILH Basis)

$$g_{Zu_L u_L}^h = \frac{g}{c_{\theta_W}} \frac{m_W^2}{\Lambda^2} (c_W + c_{HW} - c_{2W} - \frac{t_{\theta_W}^2}{3} (c_B + c_{HB} - c_{2B}))$$
$$g_{Zd_L d_L}^h = -\frac{g}{c_{\theta_W}} \frac{m_W^2}{\Lambda^2} (c_W + c_{HW} - c_{2W} + \frac{t_{\theta_W}^2}{3} (c_B + c_{HB} - c_{2B}))$$
$$g_{Zu_R u_R}^h = -\frac{4gs_{\theta_W}^2}{3c_{\theta_W}^3} \frac{m_W^2}{\Lambda^2} (c_B + c_{HB} - c_{2B})$$
$$g_{Zd_R d_R}^h = \frac{2gs_{\theta_W}^2}{3c_{\theta_W}^3} \frac{m_W^2}{\Lambda^2} (c_B + c_{HB} - c_{2B})$$

ZH: Four directions in the EFT space (Higgs Primaries Basis)

$$\begin{aligned}g_{Zu_Lu_L}^h &= 2\delta g_{Zu_Lu_L}^Z - 2\delta g_1^Z (g_f^Z c_{2\theta_W} + eQ s_{2\theta_W}) + 2\delta\kappa_\gamma g' Y_h \frac{s_{\theta_W}}{c_{\theta_W}^2} \\g_{Zd_Ld_L}^h &= 2\delta g_{Zd_Ld_L}^Z - 2\delta g_1^Z (g_f^Z c_{2\theta_W} + eQ s_{2\theta_W}) + 2\delta\kappa_\gamma g' Y_h \frac{s_{\theta_W}}{c_{\theta_W}^2} \\g_{Zu_Ru_R}^h &= 2\delta g_{Zu_Ru_R}^Z - 2\delta g_1^Z (g_f^Z c_{2\theta_W} + eQ s_{2\theta_W}) + 2\delta\kappa_\gamma g' Y_h \frac{s_{\theta_W}}{c_{\theta_W}^2} \\g_{Zd_Rd_R}^h &= 2\delta g_{Zd_Rd_R}^Z - 2\delta g_1^Z (g_f^Z c_{2\theta_W} + eQ s_{2\theta_W}) + 2\delta\kappa_\gamma g' Y_h \frac{s_{\theta_W}}{c_{\theta_W}^2}\end{aligned}$$

[Gupta, Pomarol, Riva, 2014]

ZH: Four directions in the EFT space (Universal model Basis)

$$\begin{aligned}g_{Zu_Lu_L}^h &= -\frac{g}{c_{\theta_W}} \left((c_{\theta_W}^2 + \frac{s_{\theta_W}^2}{3}) \delta g_1^Z + W + \frac{t_{\theta_W}^2}{3} (\hat{S} - \delta\kappa_\gamma - Y) \right) \\g_{Zd_Ld_L}^h &= \frac{g}{c_{\theta_W}} \left((c_{\theta_W}^2 - \frac{s_{\theta_W}^2}{3}) \delta g_1^Z + W - \frac{t_{\theta_W}^2}{3} (\hat{S} - \delta\kappa_\gamma - Y) \right) \\g_{Zu_Ru_R}^h &= -\frac{4gs_{\theta_W}^2}{3c_{\theta_W}^3} (\hat{S} - \delta\kappa_\gamma + c_{\theta_W}^2 \delta g_1^Z - Y) \\g_{Zd_Rd_R}^h &= \frac{2gs_{\theta_W}^2}{3c_{\theta_W}^3} (\hat{S} - \delta\kappa_\gamma + c_{\theta_W}^2 \delta g_1^Z - Y)\end{aligned}$$

[Franceschini, Panico, Pomarol, Riva, Wulzer, 2017]

The four dibosonic channels

Amplitude	High-energy primaries	Amplitude	High-energy primaries
$\bar{u}_L d_L \rightarrow W_L Z_L, W_L h$	$\sqrt{2} a_q^{(3)}$	$\bar{u}_L d_L \rightarrow W_L Z_L, W_L h$	$\frac{g_{Z d_L d_L}^h - g_{Z u_L u_L}^h}{\sqrt{2}}$
$\bar{u}_L u_L \rightarrow W_L W_L$ $\bar{d}_L d_L \rightarrow Z_L h$	$a_q^{(1)} + a_q^{(3)}$	$\bar{u}_L u_L \rightarrow W_L W_L$ $\bar{d}_L d_L \rightarrow Z_L h$	$g_{Z d_L d_L}^h$
$\bar{d}_L d_L \rightarrow W_L W_L$ $\bar{u}_L u_L \rightarrow Z_L h$	$a_q^{(1)} - a_q^{(3)}$	$\bar{d}_L d_L \rightarrow W_L W_L$ $\bar{u}_L u_L \rightarrow Z_L h$	$g_{Z u_L u_L}^h$
$\bar{f}_R f_R \rightarrow W_L W_L, Z_L h$	a_f	$\bar{f}_R f_R \rightarrow W_L W_L, Z_L h$	$g_{Z f_R f_R}^h$

VH and VV channels are entwined by symmetry and they constrain the same set of observables at High energies but may have different directions [Franceschini, Panico, Pomarol, Riva, Wulzer, 2017 & SB, Gupta, Reiness, Seth (in progress)]

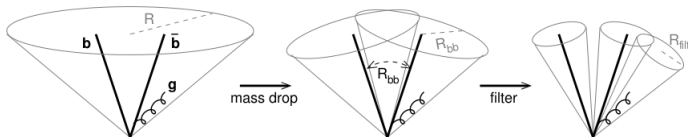


FIG. 1: The three stages of our jet analysis: starting from a hard massive jet on angular scale R , one identifies the Higgs neighbourhood within it by undoing the clustering (effectively shrinking the jet radius) until the jet splits into two subjects each with a significantly lower mass; within this region one then further reduces the radius to R_{filt} and takes the three hardest subjects, so as to filter away UE contamination while retaining hard perturbative radiation from the Higgs decay products.

Given a hard jet j , obtained with some radius R , we then use the following new iterative decomposition procedure to search for a generic boosted heavy-particle decay. It involves two dimensionless parameters, μ and y_{cut} :

1. Break the jet j into two subjects by undoing its last stage of clustering. Label the two subjects j_1, j_2 such that $m_{j_1} > m_{j_2}$.
2. If there was a significant mass drop (MD), $m_{j_1} < \mu m_{j_2}$, and the splitting is not too asymmetric, $y = \frac{\min(p_{tj_1}^2, p_{tj_2}^2) \Delta R_{j_1, j_2}^2}{m_j^2} > y_{\text{cut}}$, then deem j to be the heavy-particle neighbourhood and exit the loop. Note that $y \simeq \min(p_{tj_1}, p_{tj_2}) / \max(p_{tj_1}, p_{tj_2})$.¹
3. Otherwise redefine j to be equal to j_1 and go back to step 1.

The final jet j is to be considered as the candidate Higgs boson if both j_1 and j_2 have b tags. One can then identify R_{bb} with $\Delta R_{j_1, j_2}$. The effective size of jet j will thus be just sufficient to contain the QCD radiation from [the](#)

In practice the above procedure is not yet optimal for LHC at the transverse momenta of interest, $p_T \sim 200 - 300$ GeV because, from eq. (1), $R_{bb} \gtrsim 2m_b/p_T$ is still quite large and the resulting Higgs mass peak is subject to significant degradation from the underlying event (UE), which scales as R_{bb}^4 [16]. A second novel element of our analysis is to [filter](#) the Higgs neighbourhood. This involves resolving it on a finer angular scale, $R_{\text{filt}} < R_{bb}$, and taking the three hardest objects (subjects) that appear — thus one captures the dominant $\mathcal{O}(\alpha_s)$ radiation from the Higgs decay, while eliminating much of the UE contamination. We find $R_{\text{filt}} = \min(0.3, R_{bb}/2)$ to be rather effective. We also require the two hardest of the subjects to have the b tags.

Relevant operators

- Dimension 6 operators which modify the Higgs self-interactions

$$\mathcal{O}_{\Phi,1} = (D_\mu \Phi^\dagger) \Phi \Phi^\dagger (D^\mu \Phi) \quad \mathcal{O}_{\Phi,2} = \frac{1}{2} \partial_\mu (\Phi^\dagger \Phi) \partial^\mu (\Phi^\dagger \Phi)$$

$$\mathcal{O}_{\Phi,3} = \frac{1}{3} (\Phi^\dagger \Phi)^3 \quad \mathcal{O}_{\Phi,4} = (D_\mu \Phi^\dagger) (D^\mu \Phi) \Phi^\dagger \Phi \quad \mathcal{O}_{GG} = G_{\mu\nu}^a G^{a,\mu\nu} \Phi^\dagger \Phi$$

- $\mathcal{O}_{\Phi,2/3}$ only modify Higgs self-couplings but $\mathcal{O}_{\Phi,1/4}$ also modify HVV couplings and V masses
- $\mathcal{O}_{\Phi,1}$ contributes to m_Z and not to m_W → Violates Custodial symmetry → Strongly constrained by T -parameter → Neglected for collider studies
- Redundancy amongst operators upon using EOMs → $\mathcal{O}_{\Phi,2}$, $\mathcal{O}_{\Phi,3}$ and $\mathcal{O}_{\Phi,4}$ are not independent
- Including SM Yukawa, the operator $\mathcal{O}_{\Phi,f} = (\Phi^\dagger \Phi) \bar{L} \Phi f_R + \text{h.c.}$, where $L = (f_L^u, f_L^d)^T$ becomes relevant
- One can remove $\mathcal{O}_{\Phi,4}$ using EOMs → Left with $(\mathcal{O}_{\Phi,2}, \mathcal{O}_{\Phi,3}, \mathcal{O}_{\Phi,f}, \mathcal{O}_{GG})$

Non-linear EFT realisation

- Many popular BSM extensions which give rise to modification of Higgs interactions
- Composite Higgs models assume that the Higgs is a pNGB of a strongly coupled UV completion
- The electroweak chiral Lagrangian best describes the low-energy effects of a strongly-coupled embedding of the SM

$$\begin{aligned} \mathcal{L}^{\text{ew}\chi} \supset & - V(h) + \frac{g_s^2}{48\pi^2} G_{\mu\nu}^a G_a^{\mu\nu} \left(k_g \frac{h}{v} + \frac{1}{2} k_{2g} \frac{h^2}{v^2} + \dots \right) \\ & - \frac{v}{\sqrt{2}} (\bar{u}_L^i \bar{d}_L^i) \Sigma \left[1 + c \frac{h}{v} + c_2 \frac{h^2}{v^2} + \dots \right] \begin{pmatrix} y_{ij}^u u_R^j \\ y_{ij}^d d_R^j \end{pmatrix} + \text{h.c.}, \end{aligned}$$

with

$$V(h) = \frac{1}{2} m_h^2 h^2 + d_3 \frac{m_h^2}{2v} h^3 + d_4 \frac{m_h^2}{8v^2} h^4 + \dots$$

- Here the $SU(2) \times U(1)$ symmetry is non-linearly realised $\Sigma(x) = e^{i\sigma^a \phi^a(x)/v}$ with the Goldstone bosons ϕ^a ($a=1,2,3$) and the Pauli matrices σ^a

Non-linear EFT realisation

- 5 vertices are of imminent importance, *viz.*, k_g, k_{2g}, c, c_2, d_3 in the top-Higgs sector
- k_g and c → can be constrained from gluon-fusion, VBF, $t\bar{t}h$ production
- k_{2g}, c_2 and d_3 → can be constrained at LO from double-Higgs processes
- To over-constrain the parameter space of $\mathcal{L}^{\text{ew}\chi}$ it is necessary to access as many di-Higgs processes as possible, *viz.*, $pp \rightarrow hh, hhj, hhjj, t\bar{t}hh$
- $t\bar{t}hh$ is the only process with appreciable cross-section that has the ability to constrain c_2 at tree-level
- Here however, we will discuss in terms of the following simplified Lagrangian

$$\mathcal{L}^{\text{simp}} = \mathcal{L}^{\text{SM}} + (1 - \kappa_\lambda)\lambda_{\text{SM}}h^3 + \kappa_{t\bar{t}hh}(\bar{t}_L t_R h^2 + \text{h.c.}) - \frac{1}{8}\kappa_{\text{gg}hh}G_{\mu\nu}^a G_a^{\mu\nu}h^2,$$

where $\lambda_{\text{SM}} = \lambda v = \frac{m_h^2}{2v}$ and $\kappa_\lambda = \lambda_{\text{BSM}}/\lambda_{\text{SM}}$

Bases translations

[Giudice, Grojean, Pomarol, Rattazzi; 2007, Feruglio; 1993]

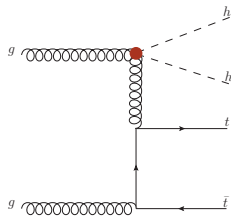
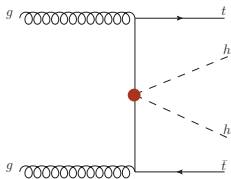
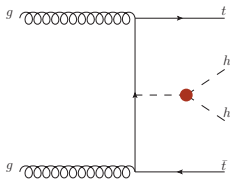
Coupling	Non-linear EFT	Simplified Lagrangian	SILH
hhh	d_3	κ_λ	$1 + (c_6 - c_\tau/4 - 3c_H/2)\xi$
$t\bar{t}hh$	c_2	$-\frac{\sqrt{2}v}{y_t}\kappa_{t\bar{t}hh}$	$-(c_H + 3c_Y + c_\tau/4)\xi/2$
$gghh$	k_{2g}	$-\frac{12\pi^2 v^2}{g_s^2}\kappa_{gghh}$	$3c_g\left(\frac{y_t^2}{g_\rho^2}\right)\xi$

Table: Relationship between the hhh , $t\bar{t}hh$ and $gghh$ vertices in three different bases, where $\xi \equiv (v/f)^2$.

$$\begin{aligned}
 \mathcal{L}_{\text{SILH}} = & \frac{\bar{c}_H}{2v^2} \partial^\mu [\Phi^\dagger \Phi] \partial_\mu [\Phi^\dagger \Phi] + \frac{\bar{c}_T}{2v^2} [\Phi^\dagger \overleftrightarrow{D}^\mu \Phi] [\Phi^\dagger \overleftrightarrow{D}_\mu \Phi] - \frac{\bar{c}_6 \lambda}{v^2} [\Phi^\dagger \Phi]^3 \\
 & - \left[\frac{\bar{c}_u}{v^2} y_u \Phi^\dagger \Phi \Phi^\dagger \cdot \bar{Q}_L u_R + \frac{\bar{c}_d}{v^2} y_d \Phi^\dagger \Phi \Phi \bar{Q}_L d_R + \frac{\bar{c}_l}{v^2} y_l \Phi^\dagger \Phi \Phi \bar{L}_L e_R + \text{h.c.} \right] \\
 & + \frac{ig}{m_W^2} \bar{c}_W [\Phi^\dagger T_{2k} \overleftrightarrow{D}^\mu \Phi] D^\nu W_{\mu\nu}^k + \frac{ig'}{2m_W^2} \bar{c}_B [\Phi^\dagger \overleftrightarrow{D}^\mu \Phi] \partial^\nu B_{\mu\nu} \\
 & + \frac{2ig}{m^2} \bar{c}_{HW} [D^\mu \Phi^\dagger T_{2k} D^\nu \Phi] W_{\mu\nu}^k + \frac{ig'}{m^2} \bar{c}_{HB} [D^\mu \Phi^\dagger D^\nu \Phi] B_{\mu\nu}
 \end{aligned}$$

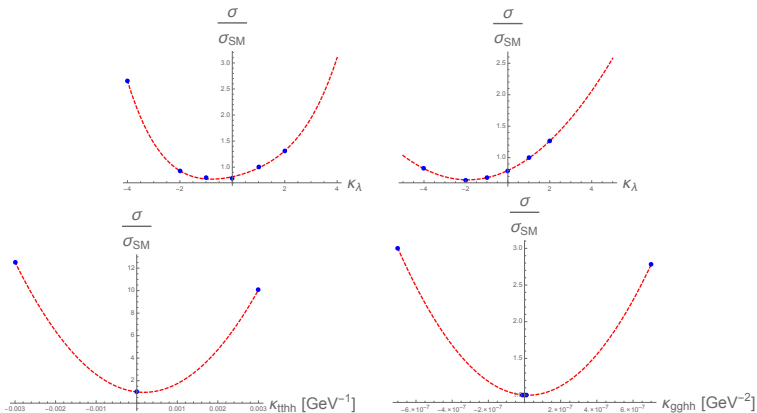
Constraining κ_λ and $\kappa_{t\bar{t}hh}$ from $t\bar{t}hh$ at 100 TeV

- Feynman diagrams showing the impact of the three effective vertices, viz., hhh , $t\bar{t}hh$ and $gghh$



Constraining κ_λ and $\kappa_{t\bar{t}hh}$ from $t\bar{t}hh$ at FCC-hh

- σ/σ_{SM} with respect to $\kappa_\lambda, \kappa_{t\bar{t}hh}, \kappa_{gggh}$
- First row shows σ/σ_{SM} at 100 TeV and at 14 TeV [Frederix *et. al.*; 2014]



Constraining κ_λ and $\kappa_{t\bar{t}hh}$ from $t\bar{t}hh$ at FCC-hh

- Unlike many di-Higgs processes, in $t\bar{t}hh$ cross-section increases with $\lambda > \lambda_{\text{SM}}$
- For κ_λ , growth of cross-section for $\lambda < 0$ has different features at 14 TeV and 100 TeV machines
- In linear EFT scenarios, the coupling modifying ggh and $gghh$ are correlated
→ In non-linear EFT they are uncorrelated
- We vary κ_λ and $\kappa_{t\bar{t}hh}$ to obtain bounds on these couplings

Constraining κ_λ and $\kappa_{t\bar{t}hh}$ from $t\bar{t}hh$ at FCC-hh

[SB, F. Krauss, M. Spannowsky; 2019]

- For $\kappa_\lambda = 1$, $\sigma_{t\bar{t}hh}^{100 \text{ TeV}} / \sigma_{t\bar{t}hh}^{14 \text{ TeV}} \sim 75$
- 14 TeV study yields ~ 13 signal events and $\kappa_\lambda \lesssim 2.5$ at 95% CL [Englert *et. al.*; 2014]
- For the 100 TeV analysis, we consider final state with 6 b -tagged jets, 1 isolated lepton, at least 2 light jets and \cancel{E}_T
- Several backgrounds at play, *viz.*, QCD processes: $t\bar{t}b\bar{b}b\bar{b}$, $t\bar{t}hb\bar{b}$, $t\bar{t}Zb\bar{b}$ and EW processes $t\bar{t}hZ$, $t\bar{t}ZZ$
- Fake backgrounds: $t\bar{t}b\bar{b} + \text{jets}$, $t\bar{t}h + \text{jets}$, $t\bar{t}Z + \text{jets}$, $W^\pm b\bar{b}b\bar{b} + \text{jet}$, $W^\pm c\bar{c}c\bar{c} + \text{jets}$, $W^\pm b\bar{b} + \text{jets}$, $t\bar{t}c\bar{c}c\bar{c}$, misidentifying c or light jets as b -tagged jets
- We assume b -tagging efficiency of 80%, 10% (1%) mistagging efficiency for c -jets (light jets)

$t\bar{t}hh$ Scale choices

Process category	μ_F^2	μ_R^2
$t\bar{t}HH, t\bar{t}ZZ, t\bar{t}HZ$ $t\bar{t}Hb\bar{b}, t\bar{t}Zb\bar{b}$	$\frac{1}{4} H_T^2 + 2m_t^2 + \{2m_H^2, 2m_Z^2, m_H^2 + m_Z^2\}$ $\frac{1}{4} H_T^2 + m_{H,Z}^2 + 2m_t^2$	$\frac{1}{4} H_T^2 + 2m_t^2$ $\frac{1}{4} H_T^2 + 2m_t^2$
$t\bar{t} + b's, c's$ or light jets	$\frac{1}{4} H_T^2 + 2m_t^2$	$\frac{1}{4} H_T^2 + 2m_t^2$
$W + b's, c's$ or light jets	$\frac{1}{4} H_T^2 + m_W^2$	$\frac{1}{4} H_T^2$

Table: Renormalisation and factorisation scales used for the various processes

Constraining κ_λ and $\kappa_{t\bar{t}hh}$ from $t\bar{t}hh$ at FCC-hh

- For the $t\bar{t}Z/h+$ jets, we consider a merged sample, where additional jets ensue from QCD radiation including the $g \rightarrow b\bar{b}$ splitting
- We ensure that the additional jets do not contain > 1 B -mesons by requiring that the B -hadron closest to the jet axis satisfies $x_B = \frac{|\vec{p}_B|}{|\vec{p}_j|} \times \frac{\vec{p}_B \cdot \vec{p}_j}{|\vec{p}_B||\vec{p}_j|} > 0.7$
- Reflects b -quark fragmentation \rightarrow Allows to suppress "doubly-tagged" b -jets
- We first reconstruct the two Higgs bosons by minimising the following χ^2

$$\chi_{HH}^2 = \frac{(m_{b_i, b_j} - m_h)^2}{\Delta_h^2} + \frac{(m_{b_k, b_l} - m_h)^2}{\Delta_h^2},$$

$i \neq j \neq k \neq l$ run over all the 6 b -tagged jets, $m_h = 120$ GeV taking into account invisible decays of B -mesons and $\Delta_h = 20$ GeV

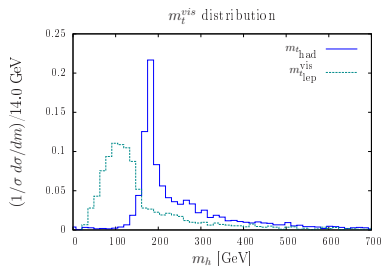
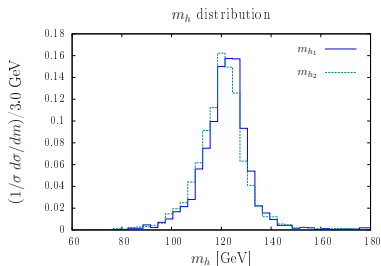
- We then require $|m_{b_i, b_j} - m_h| < \Delta_h$ and $|m_{b_k, b_l} - m_h| < \Delta_h$

Constraining κ_λ and $\kappa_{t\bar{t}hh}$ from $t\bar{t}hh$ at FCC-hh

- Then we take the 2 remaining b -jets and minimise the following χ^2

$$\chi_{t_h}^2 = \frac{(m_{b_i, j_k, j_l} - m_t)^2}{\Delta_t^2},$$

$k \neq l$ and $\Delta_t = 40$ GeV We then require $|m_{b_i, j_k, j_l} - m_t| < \Delta_t$



- Finally we require $m_{t_{lep}}^{vis} < m_t$

Constraining κ_λ and $\kappa_{t\bar{t}hh}$ from $t\bar{t}hh$ at FCC-hh

[SB, F. Krauss, M. Spannowsky; 2019]

- At the design luminosity of 30 ab^{-1} , we expect ~ 260 signal events for $\kappa_\lambda = 1$ and ~ 1900 background events, with $S/B \sim 0.14$ and statistical significance of $S/\sqrt{B} \sim 5.9$
- Upon taking $\kappa_{t\bar{t}hh} = 0$, one obtains (using the CLs method) at 68% CL with 5% (10%) systematic uncertainty

$$-3.20 < \kappa_\lambda < 2.60 \quad (-3.43 < \kappa_\lambda < 2.92) \quad 3/\text{ab}$$

$$-2.89 < \kappa_\lambda < 2.15 \quad (-3.27 < \kappa_\lambda < 2.70) \quad 30/\text{ab}$$

- Upon taking $\kappa_\lambda = 1$, one obtains (using the CLs method) at 68% CL with 5% (10%) systematic uncertainty

$$-0.59 \text{ TeV}^{-1} < \kappa_{t\bar{t}hh} < 0.95 \text{ TeV}^{-1} \quad (-0.71 \text{ TeV}^{-1} < \kappa_{t\bar{t}hh} < 1.07 \text{ TeV}^{-1}) \quad 3/\text{ab}$$

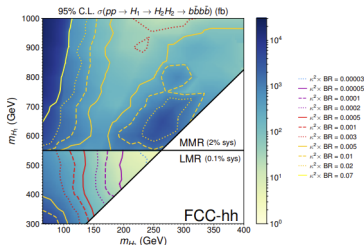
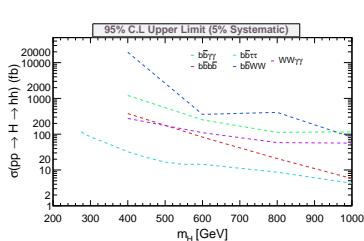
$$-0.43 \text{ TeV}^{-1} < \kappa_{t\bar{t}hh} < 0.78 \text{ TeV}^{-1} \quad (-0.63 \text{ TeV}^{-1} < \kappa_{t\bar{t}hh} < 0.99 \text{ TeV}^{-1}) \quad 30/\text{ab}$$

- Ultimate goal is to perform a global fit using the $pp \rightarrow hh$, $pp \rightarrow hhj$, $pp \rightarrow hhjj$ and $pp \rightarrow t\bar{t}hh$ with all these couplings to find correlated bounds

Resonant di-Higgs at HL-LHC and FCC-hh

- Bounds on $\sigma(pp \rightarrow H \rightarrow hh)$ at HL-LHC (left) from various channels and at FCC-hh (right) from $b\bar{b}b\bar{b}$

[A. Adhikary, SB, R. K. Barman and B. Bhattacharjee; 2018, D. Barducci, K. Mimasu, J. M. No, C. Vernieri and J. Zurita; 2019]



- Right plot: isocontours of sensitivity on $\kappa^2 \times \text{BR}$ ($\kappa^2 \times \text{BR}$ is defined by $\sigma(pp \rightarrow H_1 \rightarrow H_2 H_2 \rightarrow b\bar{b}b\bar{b}) = \hat{\sigma}_{H_1} \times \kappa^2 \times \text{BR}$ and $\hat{\sigma}_{H_1}$ is production of SM-like Higgs with mass m_{H_1})
- FCC-hh can set stringent limit on $\kappa \times \text{BR} \rightarrow$ factor ~ 40 improvement with respect to HL-LHC